NSRRC-J04418(2014)

Journal of Materials Chemistry B

PAPER

View Article Online
View Journal | View Issue

Published on 04 June 2014. Downloaded by National Chiao Tung University on 28/08/2014 09:42:29.

Cite this: J. Mater. Chem. B, 2014, 2, 5083

Water-based synthesis and processing of novel biodegradable elastomers for medical applications†

Shan-hui Hsu,*[a] Kun-Che Hung,[a] Ying-Yi Lin,[a] Chiu-Hun Su,[b] Hsi-Yi Yeh,[a] U-Ser Jeng,[c] Chun-Yi Lu,[a] Shenghong A. Dai,[d] Wei-En Fu[e] and Jui-Che Lin[f]

Received 10th April 2014
Accepted 1st June 2014

DOI: 10.1039/c4tb00572d

www.rsc.org/MaterialsB

Biodegradable elastomers in the form of polyurethane nanoparticles (NPs) were successfully synthesized based on the combinations of two hydrolysis-prone polyester diols by a green water-based process. The anionic nature of the polymers successfully rendered polyurethane NPs (30–50 nm) consisting of approximately 200–300 polymer chains. The mechanical properties and degradation rate could be adjusted by the types and ratios of the component oligodiols in the soft segment. We demonstrated the feasibility using these biodegradable NPs as building blocks to generate self-assembled morphologies in nanometric, micrometric, or bulk scale, bearing excellent elasticity and biocompatibility. The elastic NPs and their various assembled forms represent a series of smart biodegradable elastomers with potential medical applications.

Introduction

Biodegradable polymers such as polylactic acid (PLA), polyglycolic acid (PGA), poly(lactic-*co*-glycolic acid) (PLGA), and poly(ε-caprolactone) (PCL)[1,2] as well as their nanoparticles (NPs) have been popular in biomedical industries including drug delivery and medical devices. However, the elastic properties of these biodegradable polymers are often inadequate.[3,4] Generation of NPs from these polymers requires the use of organic solvent. On the other hand, many elastic polymers (*i.e.* elastomers) demonstrate good mechanical strength and creep recovery, but are non-biodegradable and have poor long-term biocompatibility.[5]

Crosslinking is a common technique to induce elasticity in biodegradable polymers, but the thermoset nature and insolubility make remolding difficult.[6] Wang *et al.*[7] reported the use of glycerol and sebacic acid monomers to synthesize a tough biodegradable elastomer (PGS) by melt polycondensation. The surface of PGS is hydrophilic. The biocompatibility of PGS evaluated by 28 day rat subcutaneous implantation indicated that PGS produced a thinner fibrous capsule than PLGA. Tubular PGS matrices also supported cell growth and protein synthesis.[8] Ameer *et al.*[9] synthesized another biodegradable polyester network, poly(1,8-octanediol-*co*-citric acid) (POC). These two new elastomers are crosslinked and the elasticity is rather limited. Besides, the insolubility makes it difficult to fabricate NPs from these polymers. Biodegradable elastomers, especially those with thermoplastic and non-toxic solvent processing abilities, are thus highly wanted.

Polyurethane (PU) elastomers are a family of tough and compliant thermoplastic elastomers with a linear structure composed of hard and soft segments. Thermoplastic PU has an immense global market of approximately one billion US dollars in 2010 with an estimated increase of >7% per year.[10] PU has been used to fabricate medical devices for many decades. Biodegradable PU can be synthesized using hydrolysis-prone polyester diols such as PCL diol,[11] PLA diol,[12] and their copolymer[13] as soft segments. The hydrolysis of PCL diol-based PU was about ten times faster than polyether diol-based PU.[14] The degradation products through hydrolysis showed no obvious cytotoxicity.[15] Most biodegradable PUs involve solvent procedures.[16] Biodegradable PU based on PCL diol and poly(1,6-hexamethylene carbonate) diol was synthesized in dimethyl sulfoxide (DMSO).[17]

Growing pollution problems have led scientists to focus on the development of greener and more sustainable synthetic processes. Solvent-free biodegradable PU was produced by bulk polymerization[18] based on more reactive aromatic toluene-2,4-

[a]Institute of Polymer Science and Engineering, National Taiwan University, Taipei, Taiwan. E-mail: shhsu@ntu.edu.tw
[b]Material and Chemical Research Laboratories, Industrial Technology Research Institute, Hsinchu, Taiwan
[c]National Synchrotron Radiation Research Center, Hsinchu, Taiwan
[d]Department of Chemical Engineering, National Chung Hsing University, Taichung, Taiwan
[e]National Measurement Laboratory, Center for Measurement Standards, Industrial Technology Research Institute of Taiwan/National Measurement Laboratory, Hsinchu, Taiwan
[f]Department of Chemical Engineering, National Cheng Kung University, Tainan, Taiwan

† Electronic supplementary information (ESI) available. See DOI: 10.1039/c4tb00572d

Published on 04 June 2014. Downloaded by National Chiao Tung University on 28/08/2014 09:42:29.

diisocyante. This PU suffered from low molecular weight and weak tensile strength (≤5.99 MPa), not counting the possible liberation of toxic aromatic amines after degradation. On the other hand, waterborne or aqueous PUs also have difficulty in achieving high molecular weight and are mainly applied as micelles, coatings, films, and adhesives because of processing limitations.[19,20] Biodegradable PU cast from aqueous emulsion often showed low elongation (≤340%).[21] Aqueous and biodegradable PU NPs have so far not been reported in the literature. Therefore, aqueous PU NPs with adequate biodegradable, biocompatibility, and elasticity, the properties of which can be further fine tuned by soft segment compositions, are highly demanded.

Herein, we describe the synthesis of novel waterborne biodegradable PU (WDPU) ionomers in the form of homogeneous NPs. The formulae involve the combinations of two hydrolysis-prone oligodiols, *i.e.* PCL diol and a choice from polyethylene butylene adipate diol (PEBA diol) or PLA diol (L-form or D,L-form), as soft segments. We demonstrate that these NPs can serve as building blocks to generate core–shell NPs, gel, microspheres, sponges (foams), films, and nanofibers by water-based green processing. The properties of WDPU including the degradation rate can be modulated by the compositions of soft segments, *i.e.* the types and ratios of the two oligodiols employed in the synthesis. They have excellent biocompatibility and biodegradability and thus may be suitable for a range of medical applications.

Materials and methods

Synthesis of PU dispersions

WDPU was synthesized from a novel water-based process.[22] The reaction scheme is shown in Fig. 1. The oligodiol employed was PCL diol (M_n 2000 Da, Sigma), or a combination of PCL diol with a second oligodiol. The second oligodiol was PEBA diol (M_n 2000 Da, Greco, Taiwan), poly(L-lactide) diol (PLLA diol, M_n 2000 Da), or poly(D,L-lactide) diol (PDLLA diol, M_n 2000 Da). The PLLA diol and PDLLA diol were first synthesized from lactide (L-lactide or D,L-lactide, Purac, Netherlands) and 1,3-propanediol at 135 °C for 8 h with 0.05% stannous octoate ($Sn(Oct)_2$) as the catalyst, and further purified in ethanol. The optical rotation ($[\alpha_D^{25}]$) of the PLLA diol and PDLLA diol was measured in chloroform (1 g dL^{-1}) at 25 °C using an automatic polarimeter (Polax-2L, ATAGO) and was recorded to be −165° and +166°, respectively. The optical purity (o.p.) of PLLA diol and PDLLA diol calculated based on the equation,[23] o.p. (%) = $[\alpha_D^{25}]/[\alpha_D^{25}]_o \times 100\%$, was 99.4% and 50.9%, respectively. Isophorone diisocyanate (IPDI, Evonik Degussa GmbH; 1 : 1.9 of –OH/–NCO) and 0.03% $Sn(Oct)_2$ were added to the stirred oligodiols and the reaction was performed at the appropriate prepolymerization temperature (T_{pre}, optimized from 75–105 °C) under nitrogen for 3 h (180 rpm). After prepolymerization, the temperature was adjusted to 75 °C. 2,2-Bis(hydroxymethyl) propionic acid (DMPA, Sigma) and a limited amount (13 mL) of methyl ethyl ketone (MEK, J.T. Baker) were added to the reactor under reflux for 1 h (180 rpm). The temperature was then allowed to drop to 50 °C. The carboxylic acid groups were neutralized by the addition of triethylamine (TEA, R.D.H.).[24] All samples were dispersed by adding deionized water (110 mL) to the neutralized prepolymer which were stirred vigorously at 1100 rpm. After the dispersion, ethylenediamine (EDA, Tedia; 1.08 : 1 of NCO/(OH + NH_2)) diluted with 110 mL of deionized water was added to the reactor under continuous stirring. The stoichiometric ratio of IPDI/oligodiols/DMPA/EDA/TEA was 3.52 : 1 : 1 : 1.52 : 1. The amount of MEK only accounted for 7% of the mixture. The residual MEK and TEA were removed by vacuum distillation (80 °C, 2 h).[25] These procedures successfully produced WDPU dispersions (pH ~ 8) with a solid content about 30%, which could be further adjusted. The weight percent of the soft segment in the final product was >65%.

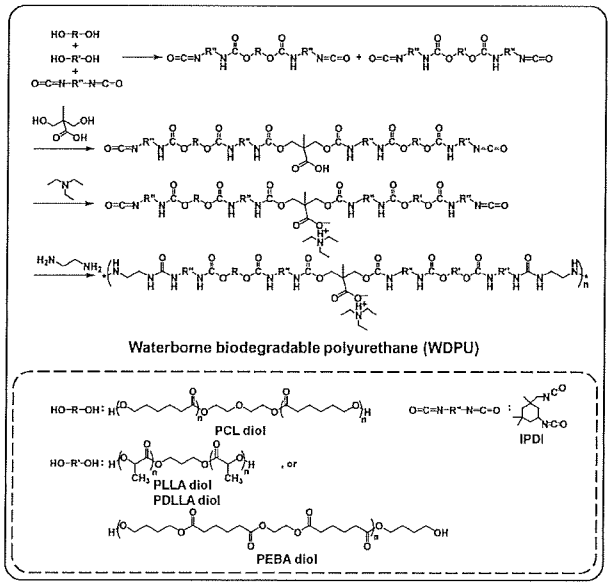

Fig. 1 Synthesis of WDPU NPs.

Physico-chemical characterization

The hydrodynamic diameter (D_h) of WDPU NPs was measured by dynamic light scattering (DLS, 165° backscatter) and the zeta potential was measured by electrophoretic light scattering, using a Delsa™ Nano C Particle Analyzer (Beckman Coulter). The diameter of gyration (D_g) and the apparent molecular weight ($M_{w,agg}$) for the unfractionated samples were investigated by the small angle X-ray scattering (SAXS) at the beamline 23A1 of the National Synchrotron Radiation Research Center (Hsinchu, Taiwan). The photon energy was set at 10 keV. The scattering vector (Q) was zero to 0.2 ($Å^{-1}$). Based on the Guinier analysis, the natural logarithm of the intensity (I) was plotted against the square of scattering vector (Q). The slope of the lowest Q-value was chosen to estimate the radius of gyration ($R_g = 0.5D_g$). Assuming monodisperse and a density of 1 g cm^{-3}, the $M_{w,agg}$ values of NPs were estimated based on the integral of Kratky function IQ^2 *vs.* Q and the intensity extrapolated to $Q = 0$, $I(0)$.[26]

This journal is © The Royal Society of Chemistry 2014

Published on 04 June 2014. Downloaded by National Chiao Tung University on 28/08/2014 09:42:29.

The hydrodynamic radius R_h ($0.5D_h$), R_g, and $M_{w,agg}$ ($M_{w,NP}$) were further analyzed by the asymmetric flow field flow fractionation (AFFFF; Eclipse™, Wyatt) followed by multi-angle light scattering (MALS), DLS, and differential refractometer (dn/dc) measurements. NPs were examined by transmission electron microscopy (TEM; JEM-1200EX II, JEOL) and atomic force microscopy (AFM; Dimension Icon™, Bruker). The diameters of NPs were measured by image analysis of the particle long axis on at least 20 NPs of different TEM images. The attenuated total reflectance-infrared (ATR-IR) spectra were collected by FTIR Spectrum 100 (Perkin Elmer) using the ATR setup. ^{1}H-Nuclear magnetic resonance (^{1}H NMR; 400 MHz, Unity Inova FT-NMR, Varian) spectra were obtained in $CDCl_3$ (20 mg mL^{-1}). M_w and M_n were determined by gel permeation chromatography (GPC; Waters) in *N*-methyl-2-pyrrolidone (NMP) using polystyrene as standards.

Control materials included a commercially available polyether-based (non-biodegradable) PU polymer, Pellethane 2363-80A (Upjohn), as well as PLA polymer (poly(D,L-lactide), M_w 121.4 kDa, low crystalline, Ingeo 2002D, NatureWorks). Pellethane films were cast from 5% solution in *N*,*N*-dimethyl acetamide. PLA films were cast from 5% solution in 1,4-dioxane. The water contact angle was measured using an FTA-1000B (First Ten Angstrom). The surface zeta potential of films was obtained using a Delsa™ Nano analyzer with a flat solid cell. *In vitro* degradation was performed according to ISO10993-13 in phosphate buffered saline (PBS) or 3% NaOH solution. The post-degradation weight was measured to determine the percent mass remaining. Degradation products were analyzed by ^{1}H NMR.

The rheological property of the gel was studied using a rheometer (SR5, Rheometric Scientific) using the cone and plate configuration at 1% shear strain and 1 Hz frequency. The mechanical properties of microspheres were determined using a nanoindentor (NanoIndenter XP, MTS). The loading force was 0.3 mN and the indentation depth was 4000 nm. The compressive or tensile strain recovery was measured by the dynamic mechanical analysis (DMA; Q-800, TA Instruments). For strain recovery, the constant-strain loading was retained for 10 s and removed. The strain of PLA and WDPU sponges (13 mm × 14 mm) was up to 30% compressive strain and that of nanofibers (15 mm × 10 mm × 0.03 mm) was up to 40% tensile strain. The tensile properties of films were analyzed at 25 °C using a universal testing instrument (HT-8504, Hung Ta) following ASTM D412-98a for elastomers (100 mm min^{-1} and 25 °C). Porosities of microspheres and sponges were measured using a gas pycnometer.

The glass transition temperature (T_g) was determined by DMA (1 Hz and 10°C min^{-1} from −100 to 150 °C) at the peak of loss tangent (tan δ (= E''/E')) curve or loss modulus (E''). The thermogravimetric analysis (TGA; TGA7, Perkin Elmer) was performed (10 °C min^{-1} under N_2) to define pyrolytic temperatures (T_{onset} at 50% weight loss and T_d at decomposition). T_g and T_m were further determined using differential scanning calorimetry (DSC; Pyris 6, Perkin Elmer; 10 °C min^{-1} −80 °C and 300 °C). X-ray diffraction (XRD; Bede D1, Bede) was conducted with the detector (2θ) scanned from 2 to 60° with a CuKα source (λ = 1.54 Å).

Materials processing

For preparing core–shell NPs, WDPU dispersions (30 wt%) were drop into 0.01% (w/v) chitosan (M_w 12 kDa and degrees of deacetylation 92.3%), and then purified using dialysis. Microspheres were prepared by a thermally induced phase separation (TIPS) process with dispersions sprayed into liquid nitrogen. The diameter of the nozzle was 350 μm and the distance from the nozzle was 20 cm. Methylene blue was loaded (16 mg per gram of microspheres) before spraying the dispersion. The amount of release in water at 37 °C was measured against time by the absorbance at 660 nm with a UV-Vis spectrometer and divided by the loaded amount (expressed as percent cumulative release). For electrospinning, WDPU dispersions were mixed with polyethylene oxide (PEO, M_w 900 kDa) in WDPU/PEO/H_2O = 12.6/5.4/82.0 wt% and placed into a syringe with a needle (23 G) that was mounted on a syringe pump at a flow rate of 10 mL h^{-1}. Randomly oriented fibers were collected by applying a high voltage (20 kV) to the needle. Sponges were freeze-dried from WDPU dispersions (5 wt%) in a Teflon dish at 20 °C for 24 h. The control PLA sponges were freeze-dried from 1,4-dioxane solution (5 wt%).

Biocompatibility evaluation *in vitro*

Adipose-derived mesenchymal stem cells were isolated from the subcutaneous fat of Sprague-Dawley rats (~350 g). The adipose tissue was cut and treated with 200 U mL^{-1} type I collagenase (Sigma) in Hank's buffered salt solution at 37 °C for 1 h with gentle agitation. Cells were collected by centrifugation, replated on T-flasks in Dulbecco's modified Eagle medium (DMEM)-low glucose/F12 (Gibco) containing 10% fetal bovine serum (FBS, Gibco) and 1% antibiotics (Invitrogen), and incubated at 37 °C with 5% CO_2. PKH26 dye (Sigma)-labeled cells were co-cultured with WDPU for 24 h. The cell density was 5 × 10^5 cells for 50 mg microspheres or 1 × 10^6 cells per sponge. Dispersion (200 μL) before gelling was mixed with 2 × 10^4 cells and incubated at 37 °C for gelation. Nanofibers (diameter 15 mm and thickness 0.03 mm) were seeded with 1 × 10^4 cells. Cell viability was further evaluated by detecting the intracellular esterase activity using calcein AM (Invitrogen).

Platelet adhesion and activation were evaluated *in vitro*.[27] Samples pre-equilibrated with HEPES-Tyrode buffer (pH 7.4) were incubated with human platelet-rich plasma (PRP, purchased from Tainan Blood Donation Center) at 37 °C under 5% CO_2 for 1 h. Specimens were rinsed thoroughly with the buffer and fixed, dehydrated, and sputter-coated for scanning electron microscopic (SEM) observation.

The responses of vascular endothelial cells and macrophages are described below. Bovine carotid artery endothelial cells (ECs) were maintained in low-glucose DMEM supplemented with 10% FBS and 1% antibiotics. Cells of passages 10–13 were used. Cell suspension (2 × 10^4 in 1 mL) was added onto each 1.5 cm diameter film placed in 24-well tissue culture plates. Cells cultured in a blank well (tissue culture polystyrene, TCPS) were used as the control. After 24 and 72 h, the adherent cells were trypsinized and counted. The gene expression of eNOS at 72 h was analyzed by reverse transcriptase-polymeric chain

Published on 04 June 2014. Downloaded by National Chiao Tung University on 28/08/2014 09:42:29.

reaction (RT-PCR) with GAPDH as the housekeeping gene. The inflammatory response was evaluated using J774A.1 murine macrophages, which were cultured in high-glucose DMEM supplemented with 10% FBS and 1% antibiotics. Cells of passages 30–40 were used. Cell seeding and culture followed those for ECs. The gene expression of inflammatory cytokines including interlukin-1 (IL-1), interlukin-6 (IL-6), and tumor necrosis factor (TNF-α) at 24 and 72 h was analyzed by RT-PCR. The macrophage size was measured using a Multisizer™ 3 Coulter Counter® (Beckman Coulter).

Rat subcutaneous implantation

All procedures followed the ethical guidelines and were approved by the Animal Care and Use Committee. Adult Sprague-Dawley rats (300–350 g) were anesthetized and a dorsal incision of ~10 mm × 10 mm was created. Samples (10 mm × 10 mm, 0.2 mm thick) were inserted into the subcutaneous sites.[28] After 29 days, a few specimens were removed and washed with deionized water containing a 1% Tween-20 surfactant, sonicated, rinsed thoroughly, and dried. The post-degradation weight and M_w were measured. The surface was examined by SEM. Specimens with surrounding tissue were fixed and stained with H&E for histological examination. The thickness of the foreign body fibrous capsule was analyzed by the software from the thinnest part of the capsule. The upper capsule thickness indicated the thickness of fibrous capsule at the skin side and the lower capsule thickness indicated that at the muscle side.

Statistical analysis

Multiple samples ($n = 3$ to 6) were gathered in each experiment and the data were expressed as mean ± standard deviation. Each experiment was repeated independently for three times to assure reproducibility. Statistical differences among the groups were determined by one way ANOVA. Results were considered statistically significant when p values were <0.05.

Results and discussion

Synthesis and NP characterization

WDPU was successfully synthesized using an optimized procedure (Fig. 1). To manipulate the elasticity, elongation, and degradation of the polymer, we selected oligodiols with different oxygen/carbon (O/C) molar ratios and structures as the soft segment compositions (smaller O/C associated with better elongation and slower degradation, while ordered structures associated with smaller elongation and slower degradation). A series of WDPU NP dispersions were prepared at the specific soft segment compositions with abbreviations indicated in Table 1. All dispersions remained unchanged at 4 °C storage for a few months. The zeta potential of all NPs was below −30 mV (Table 1), indicating stability (non-aggregation) of the dispersions.

The values of D_h obtained from DLS was 30–50 nm for different NPs (Table 1), smaller than the sizes (60–90 nm) of conventional non-degradable PU dispersions.[21,29] The values of D_g (35–50 nm) and shape factor D_g/D_h (0.9–1.1) are listed in Table 1. The ratios of D_g/D_h suggested a worm-like shape of the NPs.[30,31] The apparent molecular weight ($M_{w,agg}$) of NPs by SAXS (assuming monodisperse) was estimated to be in the range of 1–3 × 10^7 Da for various NPs (*e.g.* 2.1 × 10^7 Da for PCL100 and 2.8 × 10^7 Da for PCL40EB60).

Two WDPU (PCL100 and PCL40EB60) NPs were deliberately characterized after fractionation with AFFFF. It was found that the size distribution of NPs was rather uniform. For PCL100 NPs, the z-average D_g, z-average D_h, and weight-average $M_{w,agg}$ were 42.2 ± 0.4 nm, 42.4 ± 1.5 nm, and 4.326 × 10^7 Da (polydispersity 1.1). For PCL40EB60 NPs, these values were 45.8 ± 0.8 nm, 42.8 ± 0.6 nm, and 3.940 × 10^7 Da (polydispersity 1.1), respectively. The ratios of D_g/D_h were 0.99 (PCL100) and 1.07 (PCL40EB60). These data were close enough to those obtained on unfractionated samples (Table 1). Therefore, AFFFF analyses confirmed the homogeneity of the prepared NPs and the appropriateness of SAXS measurements on unfractionated samples. The particle density (ρ_p) estimated from D_h and $M_{w,agg}$ (*i.e.* $M_{w,NP}$) was in the range of 1.0–1.8 g cm^{-3}, indicating that the structure of each polymer NP was rather compact. The weight average molecular weight of a single polymer chain (M_w) determined by GPC was 110–190 kDa with polydispersity 1.2–1.9 (Table 1). Therefore, each NP contains ~200–300 molecules (Fig. 2b). The above characterization also suggested that molecular chains in the NPs may be compact and in distinct structures from the micelles of a block copolymer.[30,31]

The images of NPs by TEM also revealed the worm-like morphology (Fig. 2a). The average sizes obtained from image analysis of the long axis on at least twenty different TEM images were in the range of ~30–45 nm for various NPs. These size values were well matched to D_h and D_g obtained by DLS and SAXS aforementioned (Table 1), suggesting that the NPs were compact and not micellar-like.[32]

The ATR-IR spectra (Fig. 3a) of the dried NPs showed no adsorption band of N=C=O (2274 cm^{-1}).[33] The characteristic bands of WDPU were observed (3350 cm^{-1} N–H, 2850–3000 cm^{-1} C–H, 1600–1750 cm^{-1} C=O, and 1250 cm^{-1} C–O). ^{1}H NMR spectroscopy (Fig. 3b) revealed no peaks at 2.0 and 2.5 ppm, suggesting that the product was free of primary amine (–NH_2) and TEA.[34,35] Peaks associated with MEK (1.2, 2.1, and 2.6 ppm)[36] were also absent. The ionic component DMPA, though can bear negative charge, is a weak acid. By adding a neutralization agent such as TEA, the dissociation of DMPA can be promoted,[24] which helps disperse the NPs. After NP formation, TEA may be removed by vacuum distillation.[25] The triplet near 0.7–0.8 ppm (H_m) was assigned solely to the CH_3 group in the structure of IPDI (and not TEA), based on the integral ratios provided under each signal in Fig. 3b. The signal at 3.65 ppm (H_d) was assigned to the CH_2 group in the structure of IPDI, and that at 4.2 ppm (H_b) was assigned to the CH_2 group in the structure of DMPA.[35,37] On the other hand, the intensity at 1.1 ppm (H_k) was attributed to the CH_3 group in IPDI (in majority, 86%) as well as DMPA (14%). All of these peak assignments were further confirmed by comparing the integral ratios of the signals listed with the spectrum.

 This journal is © The Royal Society of Chemistry 2014

Published on 04 June 2014. Downloaded by National Chiao Tung University on 28/08/2014 09:42:29.

Table 1 The compositions and physico-chemical properties for various WDPU[a]

	Oligodiol composition (mol%)				NP dispersion (25 °C)		Polymer (GPC)			
Abbrev of WDPU	PCL diol	PEBA diol	PLLA diol	PDLLA diol	Zeta (mV)	D_h (nm) DLS	D_g (nm) SAXS	D_g/D_h	M_w (kDa)	M_w/M_n
PCL100	100	—	—	—	−58 ± 2	41.6 ± 3.4	38.1 ± 1.2	0.92	165.3	1.20
PCL80EB20	80	20	—	—	−58 ± 3	42.2 ± 5.2	50.2 ± 0.7	1.19	155.8	1.26
PCL60EB40	60	40	20	—	−62 ± 1	51.3 ± 2.5	—	—	164.9	1.30
PCL40EB60	40	60	—	—	−58 ± 2	42.0 ± 1.7	45.4 ± 1.3	1.08	141.0	1.23
PCL80LL20	80	—	20	—	−46 ± 1	33.9 ± 1.3	35.2 ± 1.8	1.04	187.1	1.93
PCL60LL40	60	—	40	—	−32 ± 1	33.6 ± 1.8	35.6 ± 1.1	1.06	142.7	1.93
PCL40LL60	40	—	60	—	−43 ± 1	—	—	—	155.0	1.88
PCL80DL20	80	—	—	20	−57 ± 4	36.0 ± 1.9	43.2 ± 0.9	1.20	111.7	1.35

[a] D_g values are based on the average of two independent SAXS measurements.

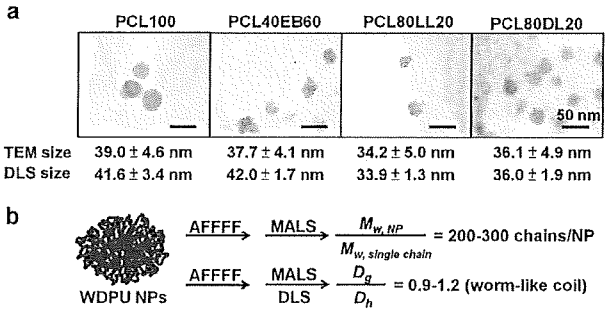

Fig. 2 (a) TEM images for various NPs. The average size calculated from TEM images was listed along with that obtained from DLS. (b) The structural characteristics of NPs, based on AFFF/MALS/DLS analyses.

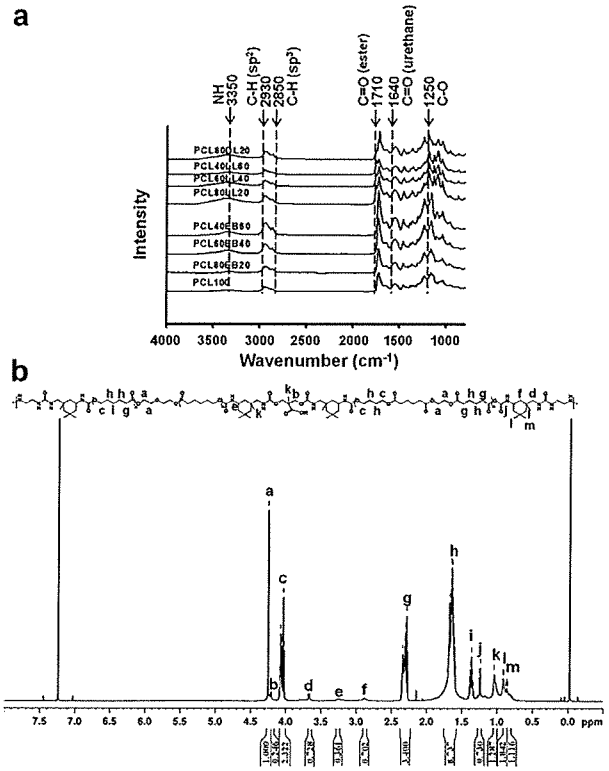

Fig. 3 Additional chemical features of WDPU. (a) The ATR-IR spectra of WDPU synthesized in this study. (b) NMR spectrum (PCL40EB60 as an example) showing no free amine and tertiary amine. The integral ratios are listed with each signal.

Water-based bottom-up of NPs into various forms

We noticed that from the WDPU NP dispersion, a wide range of nanometric, micrometric, or bulk forms could be further generated (Fig. 4a) through ionic interaction and particle assembly. First, core–shell PU–chitosan NPs (~47 nm, zeta potential ~40 mV) may be obtained facilely by dropping WDPU dispersion into chitosan solution and washed. Chitosan is a positively charged polymer with good biocompatibility. WDPU NPs in this study were negatively charged and had good mechanical properties. They were expected to form a stable polyelectrolyte complex for biomedical applications. Chitosan has been reported to cover non-biodegradable PU NPs (~62 nm) for producing anticoagulant films, but the resulting core–shell NPs were much bigger in sizes (~90–200 nm) and the properties were only studied for cast films.[29] The current core–shell NPs, smaller and biodegradable, are better suited for intravenous anticoagulants or as drug carriers. For formulae containing L-lactide or D,L-lactide, *i.e.* PCL80LL20, hydrogels may form when the solid content was above 10% and the temperature increased above 37 °C or pH decreased to 4.

All dispersions may be sprayed into liquid nitrogen to TIPS and freeze-dried to "porous" microspheres (~40% porosity). The microspheres had an average size of ~40 μm with nanopores (~350 nm). Conventional biodegradable polymers such as PLA and PLGA often rely on double-emulsion, a more complicated processing method, to obtain microspheres.[38] When the WDPU dispersion was directly freeze-dried at the solid content 1–10%, a porous sponge was generated. This scaffold fabrication method avoids the possible toxicity from the residual organic solvent. On the other hand, mixing the dispersion with <30% PEO (M_w 900 kDa) enabled the formation of nanofibers by electrospinning. So far, no biodegradable/elastic nanofibers have been fabricated from a water-based system. All WDPU dispersions, like the conventional non-degradable waterborne PU, can be cast into films, suggesting that these NPs may aggregate upon water removal. All films were transparent and

Published on 04 June 2014. Downloaded by National Chiao Tung University on 28/08/2014 09:42:29.

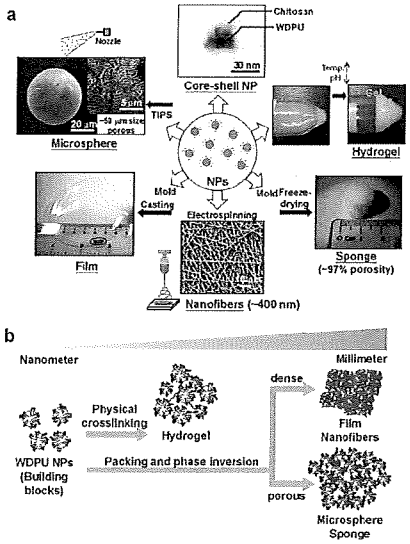

Fig. 4 Self-assembly of WDPU NPs. (a) Processing based on the self-assembly of NPs. (b) The possible mechanisms for self-assembly of NPs.

smooth with the root-mean-square roughness ~0.9–2.7 nm based on AFM topography diagrams.

The possible mechanism for self-assembly is illustrated in Fig. 4b. The temperature increase (or pH decrease) may enhance the interaction of NPs through hydrogen bonding, which plays a role in physical crosslinking and leads to gel formation.[39,40] When the concentration increases, the packing of NPs upon water removal may cause phase inversion and, with the help of soft segment chain mobility, generate a continuous phase.[41] In addition to ionic repulsion, the NPs are stabilized by hydrogen bonding between PU and water. At higher temperatures when the hydrogen bonds decrease, molecular packing may occur.[42] Moreover, the soft segment composition is critical to the structure of PU by modulating the phase segregation and chain mobility of PU. We therefore assumed that the properties, molecular packing, and self-assembly of WDPU NPs may be fine tuned by changing the combinations of soft segment, as pursued in this study. The green processes from the materials synthesis to device manufacturing are particularly advantageous for medical applications. Each of the processing methods will be explored in greater detail in the future.

Physico-chemical properties of WDPU in different forms

The properties of WDPU in different forms are illustrated in Fig. 5. In nanoscale, the three axes for a worm-like NP (PCL40EB60) estimated by AFM were 42 nm (x), 32 nm (y), and 31 nm (z) (Fig. 5a). The force–distance curve during sample detection revealed that the single NP possessed an elastic nature, though the compression modulus (~700 MPa) calculated from the force–distance curve was likely an overestimation due to the inevitable substrate effect arising from the interaction of the probe with the substrate (glass ~20 GPa).

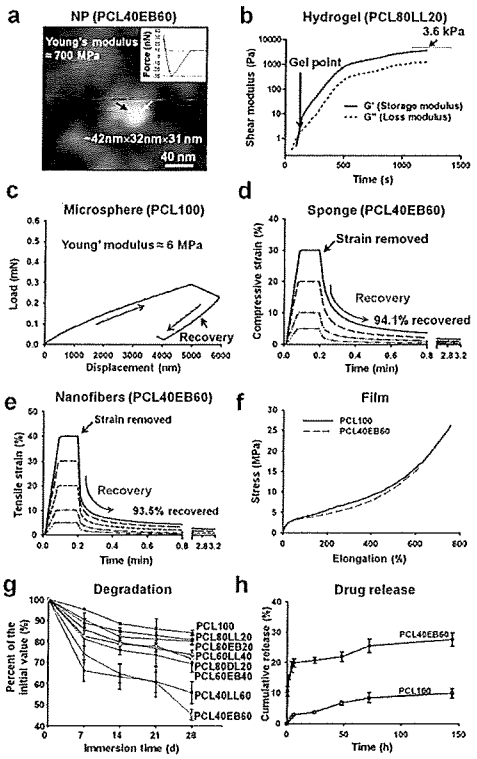

Fig. 5 Behavior of WDPU in different forms. (a) AFM image of NPs (PCL40EB60). (b) The rheology of PCL80LL20 hydrogels. (c) The elasticity of PCL100 microspheres. (d) Compressive strain recovery of PCL40EB60 sponges. (e) Tensile strain recovery of PCL40EB60 nanofibers. (f) Stress–strain curves for WDPU films. (g) Comparative *in vitro* degradation profiles of WDPU immersed in PBS at 50 °C. (h) Release profiles of methylene blue from two different microspheres.

Among various NP dispersions, the formula PCL80LL20 underwent rapid sol–gel transition (~113 s) at 37 °C and the solid content 30%. The gel was nearly cured after about 20 min (Fig. 5b). The cured gel had an elastic shear modulus (G') of ~3.6 kPa. Decreasing the solid content to <10% inhibited the gel formation. At the solid content 30%, PCL100 did not form gel even at 70 °C, while PCL80EB20 and PCL80DL20 each formed gel after ~1070 s and 500 s. In the literature, a surfactant was required for gel formation from non-biodegradable aromatic-containing PU dispersion while the gel strength was lower (~2 kPa at 40% solid content).[39] The current thermoresponsive WDPU hydrogels with tunable biodegradation rates may have potential applications as cell or drug carriers. WDPU microspheres produced facilely by TIPS were also shown to be elastic (Fig. 5c). The compression modulus measured by nanoindentation was ~6 MPa and there was apparent recovery upon decreasing force. It was possible that the deformability may favor the local delivery of microspheres by reducing the administration pressure.[43]

Freeze-dried WDPU sponges and electrospun WDPU nanofibers demonstrated good creep recovery. The DMA results as displayed in Fig. 5d and e revealed that WDPU sponges had better elastic recovery (>94% recovered) upon removal of a

 This journal is © The Royal Society of Chemistry 2014

Published on 04 June 2014. Downloaded by National Chiao Tung University on 28/08/2014 09:42:29.

compressive strain of magnitude 0.3 (30%) than sponges made from the conventional PLA polymer (only 36% recovered) (Fig. 5d). At 40% strain, WDPU sponges could still recover fairly. In addition, WDPU sponges exhibited much better wetting properties than the conventional PLA sponges (Fig. S1, ESI†). Likewise, WDPU nanofibers demonstrated >90% recovery after removal of tensile strain 40% (Fig. 5e). We also observed that these sponges and fibers possessed high elongation at break approaching 300%.

The tensile stress–strain curves of WDPU films (Fig. 5f) showed typical elastomeric behavior (25 °C and 100 mm min^{-1}). The tensile properties obtained from the curves are listed in Table S1 (in the ESI†). The Young's modulus, tensile strength, and elongation at break were in the ranges of 4.6–125 MPa, 11–35 MPa, and 280–778%, respectively. It was observed that raising the proportion of PLLA diol increased the modulus but decreased the tensile strength and elongation, which may be associated with the crystallinity of PLLA diol.[44] Replacing a part of PCL diol with 20% PDLLA diol increased the elongation and reduced the Young's modulus and tensile strength, which may be attributed to the amorphous nature of PDLLA diol.[45] The mechanical properties of WDPU were superior to those of PGS and POC in the literature (a tensile strength of 6–10 MPa and an elongation of ~260%).[7,9] For better comparisons to the existing studies[17,18,21] that conducted the tests based on ASTM D638-98 (for plastics, 10 mm min^{-1}), we repeated the tensile tests using the identical measurements (*i.e.* with a reduced rate of 10 mm min^{-1}). The strength values of WDPU were still close while the elongation increased further due to the slower stretching. For example, the elongation of PCL100 reached 923%, which was much greater than 340% reported previously for waterborne biodegradable PU.[21] The tensile strength was much better than that of solvent-free bulk polymerized biodegradable PU (≤5.99 MPa).[18] The elongation was comparable to or even greater than that of the solvent-born biodegradable PU (660–875%).[17] This evidence supported that our WDPU had superior mechanical properties.

Results from thermal analyses are shown in Fig. S2 and S3a (in the ESI†). The TGA curves demonstrated that T_d was above 300 °C for all WDPU synthesized (Fig. S2†). A summary of the TGA results is given in Table S1.† It was observed that the addition of PLLA diol or PDLLA diol reduced the pyrolytic temperatures T_{onset} and T_d, while adding PEBA diol increased them. The highest pyrolytic temperatures were observed in PCL40EB60, while the lowest were observed in PCL80DL20, probably because PDLLA diol was less thermally stable than the other oligodiols. The values of T_g were determined by DMA or DSC. The values of T_g based on DMA (tan δ and E'' curves) were in the range from −47.1 to −6.5 °C (Table S1†). As the content of PEBA diol or PLLA diol increased, T_g also increased. On the other hand, the values of T_g determined from DSC (−60.8 to −33.2 °C) were lower than those obtained from DMA and were considered as less appropriate to describe PU generally. All T_g values were well below zero, typical of elastomeric materials. No melting peak was clearly observed in DSC curves for all WDPU except the small peaks in PCL80LL20 and PCL40EB60, of which the crystallinity was ~3% and ~1% respectively (Fig. S3a†). The results of thermal analyses indicate that most WDPU is amorphous and thermoplastic. Typical XRD data are shown in Fig. S3b (in the ESI†). A broad band and the absence of peaks confirmed the lack of crystalline structure, except for PCL80LL20. Based on the XRD evaluation, PCL80LL20 was partially crystalline (~7%). The unique low crystalline character may contribute to the observed gel formation in PCL80LL20. The DSC and XRD measurements also support our hypothesis that the structure and properties of WDPU could be modulated by the types and ratios of the two oligodiols in soft segment compositions.

WDPU prepared in this study exhibited a range of degradation rates which were also controlled by the soft segment compositions. The degradation in PBS was evaluated at 50 °C for 28 days. WDPU remained 45 to 84% of the initial weight (Fig. 5g). After immersion in 3% NaOH solution at 37 °C for 24 h (accelerated degradation), the polymers remained 27 to 83% of the initial weight (Fig. S4a, ESI†). The degradation rate increased with the increased content of PEBA diol or PLLA diol. The degradation rate in PBS was ranked in the order of PCL40EB60 > PCL40LL60 > PCL60EB40 > PCL80DL20 > PCL60LL40 > PCL80LL20 ≧ PCL80EB20 > PCL100. On the other hand, the degradation rate in 3% NaOH solution was ranked in a somewhat different order (*i.e.* faster for PLA and lactide-containing WDPU), probably due to the greater resistance of PEBA diol to acidic autocatalysis. In addition, we performed the degradation of PLA in 37 °C PBS and observed that the hydrolytic degradation was rather slow for PLA compared to PCL40EB60 (Fig. S4b, ESI†). The better hydrophilicity as well as the ionic nature may account for the faster hydrolytic degradation of WDPU in PBS. The degradation product of WDPU contained mostly soft segment (Fig. S4c, ESI†). The novel WDPU polymers demonstrate tunable degradation rates which are important for their biomedical applications. The potential of WDPU as a drug carrier was verified by the slow release of a model drug, methylene blue (Fig. 5h), which was conveniently encapsulated within microspheres before spraying. There was a burst release followed by a steady release, depending on the degradation rate of the WDPU.

Biocompatibility and blood compatibility tests *in vitro*

To evaluate the biocompatibility of WDPU, we performed the cell culture test using the adipose-derived mesenchymal stem cells. The stem cells were effectively seeded in hydrogels, microspheres, sponges, and nanofibers, owing to the hydrophilicity of the materials. The cells remained alive after 24 h (Fig. 6a, shown as fluorescent cells). The non-toxicity warranted their potential applications as cell carriers. The conventional PLA polymer sponges are more hydrophobic (as shown in Fig. S1†) and usually requires pre-wetting for such applications.

In addition to the biocompatibility, the blood compatibility of WDPU was also evaluated. It was noted that human blood platelets were not activated on WDPU films (Fig. 6b). The number of platelets adhered on WDPU was significantly lower than that on the commercial non-biodegradable PU (Pellethane) (Fig. 6c). Platelets were activated with pseudopodia on the

Published on 04 June 2014. Downloaded by National Chiao Tung University on 28/08/2014 09:42:29.

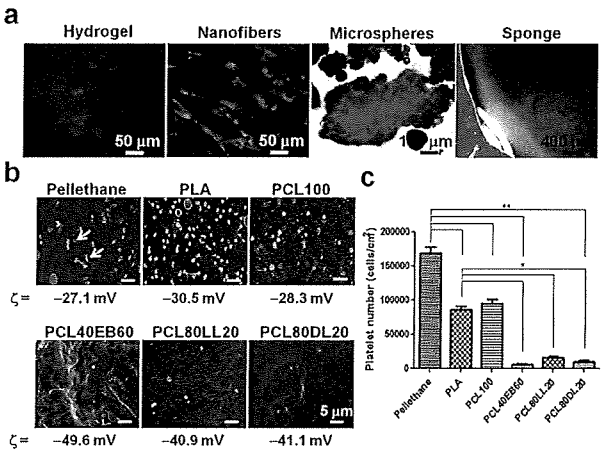

Fig. 6 Biocompatibility and biodegradation of WDPU. (a) Fluorescent images of mesenchymal stem cells co-cultured with various forms of WDPU. Cells were labeled with calcein AM (green) or PKH26 (red). Microspheres/sponges had green autofluorescence so PKH26-labeled images were shown. Nanofibers and sponges were made of PCL40EB60; hydrogels were made of PCL80LL20; and microspheres were made of PCL100. (b) SEM images showing low platelet activation on various WDPU films (surface zeta potential ζ listed) compared to the conventional Pellethane elastomer and PLA polymer. (c) Quantification for the number of platelets adhered on WDPU films. $p < 0.05$, *lower than PLA; **lower than Pellethae.

conventional PLA polymer, but were not activated on PCL40EB60, PCL80LL20, and PCL80DL20. The surface zeta potential of WDPU (listed with each panel in Fig. 6b) was more negative (except PCL100) than that of PLA or Pellethane. The low blood platelet activation by WDPU may be attributed to the rather negative surface charge (<40 mV) as the zeta potential of vascular endothelium is −42 mV.[46]

Additional biocompatibility data on the responses of vascular endothelial cells and macrophages are shown in Fig. S5 (in the ESI†). Endothelial cell attachment and proliferation on WDPU were significantly greater than those on the non-biodegradable PU (Pellethane) and were similar to those on the conventional PLA polymer. Moreover, the expression of endothelial nitric oxide synthase (eNOS) gene on WDPU was significantly greater than that on TCPS (control materials) and PLA, which indicated the correct cell phenotype and ability to promote the endothelialization of blood vessels. Macrophages were used to predict the inflammatory or immune response to WDPU. It was observed that the average size of macrophages on WDPU was slightly lower than those cultured on TCPS and Pellethane. The proinflammatory gene (IL-1, IL-6, and TNF-α) expression was similarly low for macrophages on TCPS and WDPU, *i.e.* a minimal immune reaction of WDPU. Taken together, these data suggest that the green PU developed is superior to the conventional biodegradable polymer (PLA) in biocompatibility.

Biodegradation and biocompatibility in the rat subcutaneous model

The biodegradation and biocompatibility of WDPU were verified by animal implantation. WDPU films had smooth surface before implantation (Fig. 7a). While PLA films turned opaque after 29 day rat subcutaneous implantation, WDPU films remained translucent with randomly localized opaque spots (Fig. 7b). Retrieved samples maintained the integrity, in spite of evident degradation. SEM images showed white circles and small pits on PCL100, PCL80LL20, and PCL80DL20, extensive flaking on PCL40EB60, and large round-shaped pits on PLA. The percent mass remaining was 55–88% and M_w decreased to 20–65% of the initial values (Fig. 7c). The rate of degradation *in vivo* was PLA ~ PCL80DL20 > PCL80LL20 ~ PCL40EB60 > PCL100, consistent with that predicted *in vitro*. This also suggested that the degradation mechanism of WDPU was mainly hydrolysis *in vivo*.[47] After 29 days, PCL80DL20 remained 56% of the initial mass, but M_w accounted for only 22% of the initial value. PCL80DL20 and PLA lost the most mass and M_w. The faster degradation of PCL80DL20 may be attributed to the presence of PDLLA diol that released acidic degradation products and promoted the degradation of PCL diol *in vivo*.

In the literature, the degradation rate of PCL was about three times slower than that of PDLLA; and PCL copolymerization with other lactones (*i.e.* PLA or PGA) may enhance the

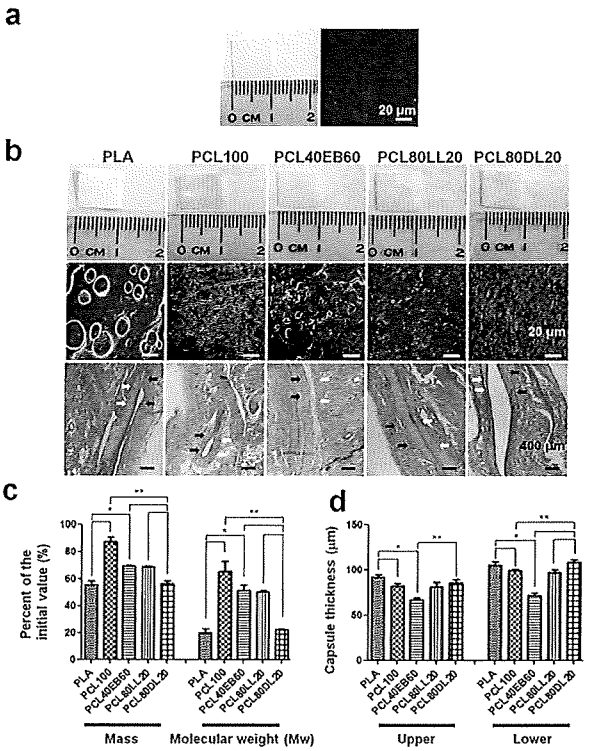

Fig. 7 (a) The gross appearance and SEM image for PCL100 before implantation. (b) The gross appearances and SEM images for samples after implantation, as well as the histology of the surrounding tissue. The white arrows (in histology) indicate the lower (muscle) side, and the white arrows indicate the upper (skin) side. (c) *In vivo* degradation (after 29 days) expressed as the percent toward the initial mass value and M_w. *$p < 0.05$, higher than PLA; **higher than PCL80DL20. (d) The foreign body reaction represented by the capsule thickness in the upper and lower sides from histology. *$p < 0.05$, lower than PLA; **lower than PCL80DL20.

This journal is © The Royal Society of Chemistry 2014

Published on 04 June 2014. Downloaded by National Chiao Tung University on 28/08/2014 09:42:29.

degradation rate.[48] The fibrous capsules for all WDPU were thinner than or comparable to that of PLA (Fig. 7d). The slightly larger capsule thickness for all samples at the lower (muscle) side was in accordance with the common observations.[49] The capsule thickness for PLA was ~100 μm, agreeing with the literature.[50] The above *in vivo* data further support the good biocompatibility of WDPU.

Biodegradable WDPU elastomers prepared and reported here are not crosslinked and have a thermoplastic nature. These features are distinct from the previously reported biodegradable elastomers PGS and POC, which are networks of ester covalent bonds (thermoset) and are insoluble.[5,7] Former water-based PUs often used NMP instead of MEK[51] and had low elongation (≤340%) probably because of larger colloidal particles.[52] Other biodegradable PUs involved toxic aromatic isocyanate, possessed limited tensile strength (≤5.99 MPa),[18] and were only soluble in strong organic solvents for further processing.[17] Although the PU developed by us was also soluble only in strong solvents (such as DMSO and NMP), the novel process allowed the dispersed NPs to self-assemble and be further processed without any inconvenience. None of the existing work has generated a "nanoelastomer" or self-assembly system facilitating the subsequent green and water-based fabrication. In the current study, even the highly (~97%) porous WDPU matrix demonstrates elastomeric behavior with good elongation (~300%) and recovery. This good elongation is similar to that of natural tissues such as arteries/veins (>260%)[52] and in contrast to the limited elongation (<10%) of porous PLA.

In summary, the water-based biodegradable NP platform shows versatility in making a variety of biodegradable/elastic prototypes. Their properties can be tuned by soft segment compositions, which involve the use of two distinct degradable oligodiols in different ratios. With the good biocompatibility, these NPs and their various self-assembled/processed forms may have a range of biomedical applications.

Conclusions

Biodegradable PU NPs with tunable degradation rates are successfully synthesized from a water-based process. The green manufacturing process can reduce the use of organic solvents and crosslinking agents. The homogeneous NPs can easily self-assemble into hydrogels, microspheres, nanofibers, sponges, and films. They have excellent elasticity and recovery (even in porous forms), as well as good cell affinity, low platelet adhesion/activation, and negligible inflammatory/immune responses. We consider that the biodegradable elastomers developed are biocompatible and have tunable properties by adjusting the soft segment combinations, which may have promise for a range of biomedical device applications.

Acknowledgements

This work was supported by the National Research Program for Nanoscience and Nanotechnology (101-2120-M-002-002) and the Program for Stem Cell and Regenerative Medicine Frontier Research (102-2321-B-002-033) sponsored by the Ministry of Science and Technology, Taiwan, R.O.C. We also thank Cheng-Yen Lin, Meng-Chao Tsai, Chun-Wei Ou, and Yan-Ping Chen for their technical help.

References

1 B. D. Ulery, L. S. Nair and C. T. Laurencin, *J. Polym. Sci., Part B: Polym. Phys.*, 2011, **49**, 832–864.
2 Y. Dong, S. Liao, M. Ngiam, C. K. Chan and S. Ramakrishna, *Tissue Eng., Part B*, 2009, **15**, 333–351.
3 L. S. Nair and C. T. Laurencin, *Prog. Polym. Sci.*, 2007, **32**, 762–798.
4 M. C. Serrano, E. J. Chung and G. A. Ameer, *Adv. Funct. Mater.*, 2010, **20**, 192–208.
5 J. Chlupac, E. Filova and L. Bacakova, *Physiol. Res.*, 2009, **58**, 119–139.
6 Y. Zhang, E. A. Matsumoto, A. Peter, P.-C. Lin, R. D. Kamien and S. Yang, *Nano Lett.*, 2008, **8**, 1192–1196.
7 Y. Wang, G. A. Ameer, B. J. Sheppard and R. Langer, *Nat. Biotechnol.*, 2002, **20**, 602–606.
8 J. Gao, A. E. Ensley, R. M. Nerem and Y. Wang, *J. Biomed. Mater. Res., Part A*, 2007, **83**, 1070–1075.
9 J. Yang, A. R. Webb and G. A. Ameer, *Adv. Mater*, 2004, **16**, 511–516.
10 Thermoplastic Polyurethane (TPU) Market – Global Industry Analysis, Market Size, Share, Trends, Analysis, Growth And Forecast, 2012–2018, Transparency Market Research, 2012.
11 F. Khan, S. Valere, S. Fuhrmann, V. Arrighi and M. Bradley, *J. Mater. Chem. B*, 2013, **1**, 2590–2600.
12 J.-B. Zeng, Y.-D. Li, Q.-Y. Zhu, K.-K. Yang, X.-L. Wang and Y.-Z. Wang, *Polymer*, 2009, **50**, 1178–1186.
13 D. Cohn and A. H. Salomon, *Biomaterials*, 2005, **26**, 2297–2305.
14 R. S. Labrow, D. J. Erfle and J. P. Santerre, *Biomaterials*, 1996, **17**, 2381–2388.
15 L. Tatai, T. G. Moore, R. Adhikari, F. Malherbe, R. Jayasekara, I. Griffiths and P. A. Gunatillake, *Biomaterials*, 2007, **28**, 5407–5417.
16 S. A. Guelcher, *Tissue Eng., Part B*, 2008, **14**, 3–17.
17 Y. Hong, J. Guan, K. L. Fujimoto, R. Hashizume, A. L. Pelinescu and W. R. Wagner, *Biomaterials*, 2010, **31**, 4249–4258.
18 N. Teramoto, Y. Saitoh, A. Takahashi and M. Shibata, *J. Appl. Polym. Sci.*, 2010, **115**, 3199–3204.
19 M. Ding, J. Li, H. Tan and Q. Fu, *Soft Matter*, 2012, **8**, 5414–5428.
20 O. Jaudouin, J.-J. Robin, J.-M. Lopez-Cuesta, D. Perrin and C. Imbert, *Polym. Int.*, 2012, **61**, 495–510.
21 A. A. de Oliveira, S. M. de Carvalho, M. de F. Leite, R. L. Oréfice and M. de M. Pereira, *J. Biomed. Mater. Res., Part B*, 2012, **100**, 1387–1396.
22 Taiwanese patents (I427091 approval and 102100076 pending) and U.S. patent application (13/317,651) (Biodegradable and biocompatible waterborne polyurethane).
23 Q. Yi, X. Wen, L. Li, B. He, Y. Nie, Y. Wu, Z. Zhang and Z. Gu, *Eur. Polym. J.*, 2009, **45**, 1970–1978.

Published on 04 June 2014. Downloaded by National Chiao Tung University on 28/08/2014 09:42:29.

24 J. Bullermann, S. Friebel, T. Salthammer and R. Spohnholz, *Prog. Org. Coat.*, 2013, **76**, 609–615.
25 Q. Zhu, Y. Wang, M. Zhou, C. Mao, X. Huang, J. Bao and J. Shen, *J. Nanosci. Nanotechnol.*, 2012, **12**, 4051–4056.
26 H. Fischer, M. de Oliveira Neto, H. B. Napolitano, I. Polikarpov and A. F. Craievich, *J. Appl. Crystallogr.*, 2010, **43**, 101–109.
27 J. M. H. Kuijpens, G. A. Kardaun, R. Blezer, A. P. Pijpers and L. H. Koole, *J. Am. Chem. Soc.*, 1995, **117**, 8691–8697.
28 S. Hsu, C. M. Tang and H. J. Tseng, *Acta Biomater.*, 2008, **4**, 1797–1808.
29 D. Xu, K. Wu, Q. Zhang, H. Hu, K. Xi, Q. Chen, X. Yu, J. Chen and X. Jia, *Polymer*, 2010, **51**, 1926–1933.
30 L. Liu, K. Xu, H. Wang, P. K. J. Tan, W. Fan, S. S. Venkatraman, L. Li and Y.-Y. Yang, *Nat. Nanotechnol.*, 2009, **4**, 457–463.
31 S. Liu, Y. I. González, D. Danino and E. W. Kaler, *Macromolecules*, 2005, **38**, 2482–2491.
32 X. Li, K. Y. Mya, X. Ni, C. He, K. W. Leong and J. Li, *J. Phys. Chem. B*, 2006, **110**, 5920–5926.
33 R. M. Versteegen, R. P. Sijbesma and E. W. Meijer, *Angew. Chem., Int. Ed.*, 1999, **38**, 2917–2919.
34 W. C. Hung, M. D. Shau, H. C. Kao, M. F. Shih and J. Y. Cherng, *J. Controlled Release*, 2009, **133**, 68–76.
35 S. Zhang, L. Cheng and J. Hu, *J. Appl. Polym. Sci.*, 2003, **90**, 257–260.
36 H. N. Cheng, T. Asakura, A. D. English, *NMR Spectroscopy of Polymers: Innovative Strategies for Complex Macromolecules*, American Chemical Society, Washington D.C., 2011.
37 C.-Y. Lee, J.-W. Kim and K.-D. Suh, *J. Mater. Sci.*, 1999, **34**, 5343–5349.
38 F. Qia, J. Wu, Q. Fan, F. He, G. Tian, T. Yang, G. Ma and Z. Su, *Colloids Surf., B*, 2013, **112**, 492–498.
39 A. S. Hoffman, *Adv. Drug Delivery Rev.*, 2002, **43**, 3–12.
40 S. A. Madbouly and J. U. Otaigbe, *Macromolecules*, 2006, **39**, 4144–4151.
41 L. K. Sawa, B. W. Brooks, K. J. Carpenter and D. V. Keight, *J. Colloid Interface Sci.*, 2004, **279**, 235–243.
42 Y. Wang, G. Wu, X. Li, Y. Wang, H. Gao and J. Ma, *J. Biomater. Sci., Polym. Ed.*, 2013, **24**, 1676–1691.
43 S. A. Bencherif, R. W. Sands, D. Bhatta, P. Arany, C. S. Verbeke, D. A. Edwards and D. J. Mooney, *Proc. Natl. Acad. Sci. U. S. A.*, 2012, **109**, 19590–19595.
44 W. Wang, P. Ping, X. Chen and X. Jing, *Eur. Polym. J.*, 2006, **42**, 1240–1249.
45 S. Mondal and J. L. Hu, *Polym. Eng. Sci.*, 2008, **48**, 233–239.
46 F. Tong, X. Chen, L. Chen, P. Zhu, J. Luan, C. Mao, J. Bao and J. Shen, *J. Mater. Chem. B*, 2013, **1**, 447–453.
47 Q. Guo, Z. Lu, Yi. Zhang, S. Li and J. Yang, *Acta Biochim. Biophys. Sin.*, 2011, **43**, 433–440.
48 Y. Wang, C. Ruan, J. Sun, M. Zhang, Y. Wu and K. Peng, *Polym. Degrad. Stab.*, 2011, **96**, 1687–1694.
49 S. Hsu, H. J. Tseng and Y. C. Lin, *Biomaterials*, 2010, **31**, 6796–6808.
50 T. M. Filion, J. Xu, M. L. Prasad and J. Song, *Biomaterials*, 2011, **32**, 985–991.
51 S. M. Cakić, M. Špírková, I. S. Ristić, J. K. B-Simendić, M. M-Cincović and R. Poręba, *Mater. Chem. Phys.*, 2013, **138**, 277–285.
52 M. C. Lee and R. C. Haut, *J. Biomech.*, 1992, **25**, 925–927.

This journal is © The Royal Society of Chemistry 2014